Bulletin of the Seismological Society of America, Vol. 101, No. 4, pp. 1971–1975, August 2011, doi: 10.1785/0120100256

Comment on "*P*-Wave Back-Azimuth and Slowness Anomalies Observed by an IMS Seismic Array LZDM" by Chunyue Hao and Zhong Zheng

by Lei Li

Abstract At the LZDM seismic array, Hao and Zheng (2010) observed extremely large back-azimuth and slowness deviations for teleseismic *P* waves, the maximum values of which were 87.1° for back-azimuth deviation and 8.68 s/° for slowness deviation. Hao and Zheng argued that the majority of the observed back-azimuth and slowness deviations could be attributed to a 9°-dip Moho beneath the LZDM array, which seems to be too small to produce the observed large deviations. The purpose of this comment is to show that their forward modeling of the back-azimuth and slowness deviations caused by dipping interface is incorrect, which as a result, gives rise to a seriously underestimated dip angle. The true attitude of the dipping interface is extracted from the observed zero-slowness rays. Assuming the same *P*-wave velocities as those used by Hao and Zheng (2010), a northeast-dipping interface with a dip of 57° is obtained. The theoretical back-azimuth and slowness deviations for this mode with greater dip calculated by a validated forward modeling program appear to be more consistent with the observed deviations. It is also argued that despite the consistency, previous studies of explosion seismology and receiver function in this area do not support such a steep northeast-dipping Moho interface. The dip interface is more likely to be located in the shallow crust. More information and further investigations are necessary to draw a final conclusion.

Introduction

Dipping subsurface structure can make the transmitted seismic waves deviate from the sagittal plane, and consequently, the back azimuth and slowness observed at the receiver are different from the theoretical values. Recently, Hao and Zheng (2010) observed significant deviations of back azimuth and slowness for teleseismic *P* waves recorded by the LZDM array. The maximum deviation observed is 87.1° in back azimuth and 8.68 s/° in slowness.

Hao and Zheng (2010) argued that the majority of the observed deviations can be attributed to a northeast-dipping Moho. To search for the strike and dip angle of the Moho, they followed the formulae given by Niazi (1966) to model the theoretical back-azimuth and slowness deviations caused by a dipping interface, and then compared the synthetic results with the observed deviations. The ratio of *P*-wave velocities above and below the Moho interface was fixed at 0.84 during their grid search (see the paragraph below their figure 9; the *P*-wave velocity is 6.8 km/s above and 8.06 km/s below the interface). They found a best-fit model with a strike of 115° and a dip angle of 9° (see their table 2). The theoretical back-azimuth and slowness deviations for their best-fit model were not shown explicitly in their paper. However, by comparing the back-azimuth residuals with and without correction in their figure 6, one can determine that the theoretical back-azimuth deviation must be over 60°. It seems unbelievable that a 9°-dip interface can produce such large deviations.

It is interesting to compare their best-fit model to the model in table 6 of Niazi (1966), the dip angle of which is 8° and the velocity ratio of which is 0.8, both close to the parameters of the model of Hao and Zheng (2010). It can be seen from figures 3, 5, and 8 of Hao and Zheng (2010) that the majority of the theoretical slowness values for the events analyzed in their paper fall in the range of 5–11 s/°, corresponding to an incidence angle from 21° to 53° in the uppermost mantle. However, one can see from table 6B of Niazi (1966) that the theoretical back-azimuth deviation for the incidence angle above 20° is at most 6°, far lower than the value shown in figure 6 of Hao and Zheng (2010). It is most likely that the forward modeling code of Hao and Zheng (2010) is incorrect and thus resulted in an unreasonable dipping-Moho model.

In this article, a new forwarding modeling program is developed. To validate the program, some numerical tests

are made using the dipping interface models given by Otsuka (1966) and Koch and Kradolfer (1997). After the validation, the theoretical back-azimuth and slowness deviations for the dip-Moho model proposed by Hao and Zheng (2010) are computed and compared with the observed deviations. Afterwards, a simple method is proposed to evaluate the true dip angle of the Moho beneath the LZDM array from the observed deviations.

Forward Modeling

The forward modeling procedure is simply an application of Snell's law. Details about the formulae used for modeling can be found in many references (e.g., Niazi, 1966; Otsuka, 1966). The input parameters needed in the calculation include the strike (or dip direction) and dip angle of the dipping interface, the wave velocities above and below the interface, and the back-azimuth and incidence angles of the incident plane waves.

To validate our newly developed program, some published models of dipping interface are chosen for numerical tests. The first group of models consists of the three models used in figure 4 of Otsuka (1966). The models have the same parameters except the dip angles, which are 10°, 15°, and 20°, respectively. The down-dip direction is N75°E. The *P*-wave velocities above and below the dipping interface are 6.7 km/s and 8.0 km/s, respectively. The incidence angle for seismic waves propagating in the lower medium is fixed at 21°. The calculated back-azimuth deviations are plotted in Figure 1a and the slowness deviation in Figure 1b; these are all consistent with the results shown in figure 4 of Otsuka (1966). The second group of models consists of the two models used in figure 8 of Koch and Kradolfer (1997). The first model is a dipping-Moho interface with a strike of 220° and a dip angle of 35°. The *P*-wave velocities above and below the Moho interface are 6.0 km/s and 8.0 km/s, respectively. The incidence angles for seismic waves in the uppermost mantle are 20° and 40°. The second model is a 12°-dip interface in the shallow crust, with a strike of 220°. The *P*-wave velocities above and below the interface are 3.5 km/s and 6.0 km/s, respectively. The incidence angles are 14° and

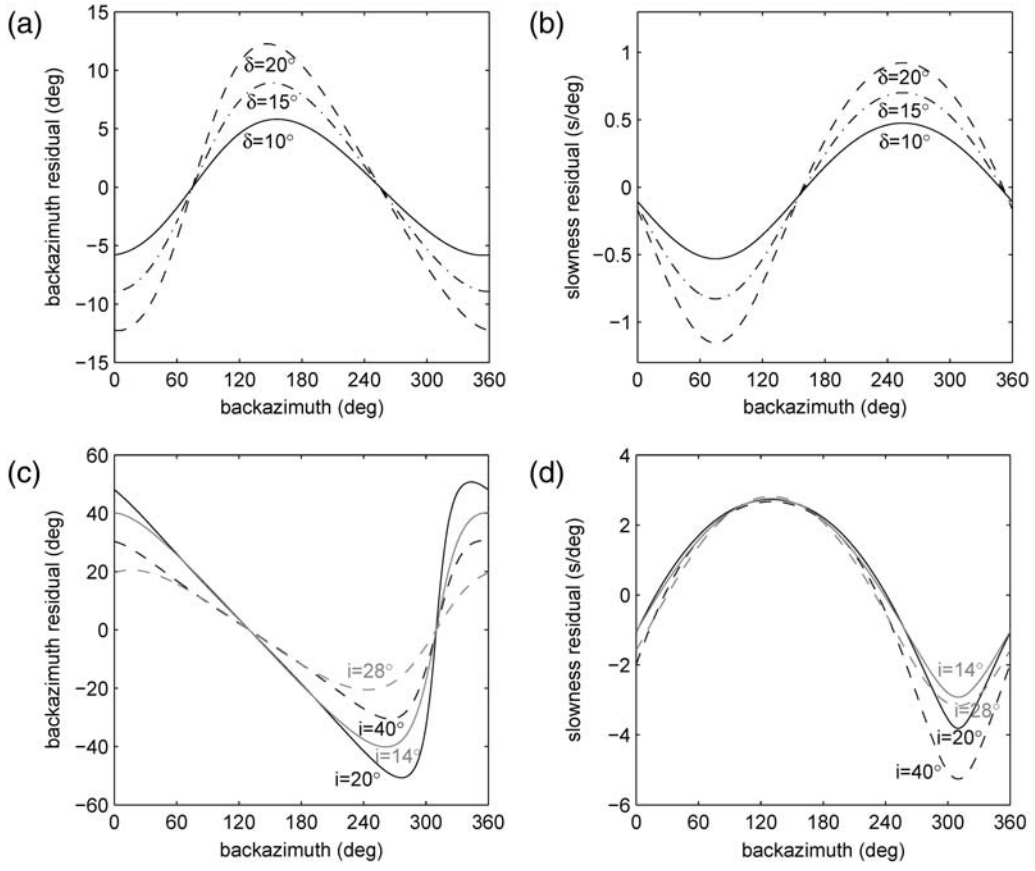

Figure 1. (a) Back-azimuth residuals and (b) slowness residuals for the three models used in figure 4 of Otsuka (1966) with an incidence angle of 21°, a *P*-wave velocity of 6.7 km/s above the interface and 8.0 km/s below the interface, a down-dip direction of N75°E, and dip angles of 10°, 15°, and 20°. (c) Back-azimuth residuals and (d) slowness residuals for the two models used in figure 8 of Koch and Kradolfer (1997). The black lines are the results for the first model, with incidence angles of 20° and 40°, a *P*-wave velocity of 6.0 km/s above the interface and 8.0 km/s below the interface, a strike of 220°, and a dip angle of 35°. The gray lines are the results for the second model, with incidence angles of 14° and 28°, a *P*-wave velocity of 3.5 km/s above the interface and 6.0 km/s below the interface, a strike of 220°, and a dip angle of 12°.

28°. The theoretical back-azimuth and slowness deviations calculated are plotted as black lines for the first model and gray lines for the second model in Figure 1c–d, which again coincide with the results shown in figure 8 of Koch and Kradolfer (1997).

After the validation, the theoretical back-azimuth and slowness deviations for the 9°-dip model proposed by Hao and Zheng (2010) are calculated and plotted in Figure 2. The model parameters are a dip angle of 9°, a down-dip direction of N25°E, a *P*-wave velocity of 6.8 km/s above the interface and 8.06 km/s below the Moho interface, and incidence angles of 21°, 35°, and 53°. It can be seen that the maximum back-azimuth deviation is no more than 5° and the maximum slowness deviation is merely 0.7 s/°, much lower than the observed deviations at the LZDM array as well as the theoretical deviations modeled by Hao and Zheng (2010). Thus, it appears that the forward modeling program of Hao and Zheng (2010) and their 9°-dip Moho model are incorrect. Hao and Zheng (2010) also proposed other dip-Moho models called submodels (see their table 5 and figures 11–14). However, the submodels are incorrect for the same reason.

Large-Dip Model

In this section, we propose a simple method to evaluate the attitude of the dipping Moho from the zero-slowness rays. From Snell's law, we know that for an incident wave coming from the down-dip direction, the refracted wave propagates vertically upward as long as the following equation:

$$\frac{\sin\delta}{v_1} = \frac{\sin(i+\delta)}{v_2}, \tag{1}$$

where δ is the dip angle, v_1 and v_2 the wave velocities above and below the interface, and i the incidence angle, is satisfied (see Figure 3 for illustration). Solving δ from equation (1) yields

$$\delta = \arctan\frac{\sin i}{v_1^{-1}v_2 - \cos i}. \tag{2}$$

Equation (2) can also be rewritten as

$$\delta = \arctan\frac{p}{v_1^{-1} - \sqrt{v_2^{-2} - p^2}}, \tag{3}$$

where $p = v_2^{-1}\sin i$ is the theoretical slowness.

It can be seen from figures 3, 5, and 8 of Hao and Zheng (2010) that for the teleseismic *P* waves coming from the northeast direction, the estimated values of slowness almost vanish, implying that the wavefront arrives at the array nearly vertically. From Figure 3, we know that the inclined interface beneath the LZDM array is down-dip toward the northeast (we assume the dip direction to be N45°E in the latter modeling). The dip angle can be calculated from equation (2) or (3). Substituting $v_1 = 6.8$ km/s, $v_2 = 8.06$ km/s, and $p = 7$ s/° into equation (3) produces $\delta = 57°$, a large dip angle far beyond the value of 9° proposed by Hao and Zheng (2010). The theoretical back-azimuth and slowness deviations for this large-dip model are plotted in Figure 4, and are visually analogous to the observed back-azimuth and slowness deviations shown in figures 4, 6, and 9 of Hao and Zheng (2010).

Discussion

There are three points to mention. Firstly, the attitude of the steep interface in this article was roughly evaluated by a visual check of the plots given by Hao and Zheng (2010). To obtain a more accurate result, formal inversion on the observation data is necessary. Secondly, the altitude difference between the elements of the LZDM array can reach up to 15% of its aperture (Xu *et al.*, 2006). Including only the horizontal slowness components in the *f*-*k* analysis can give rise to significant biases in the estimation of back azimuth

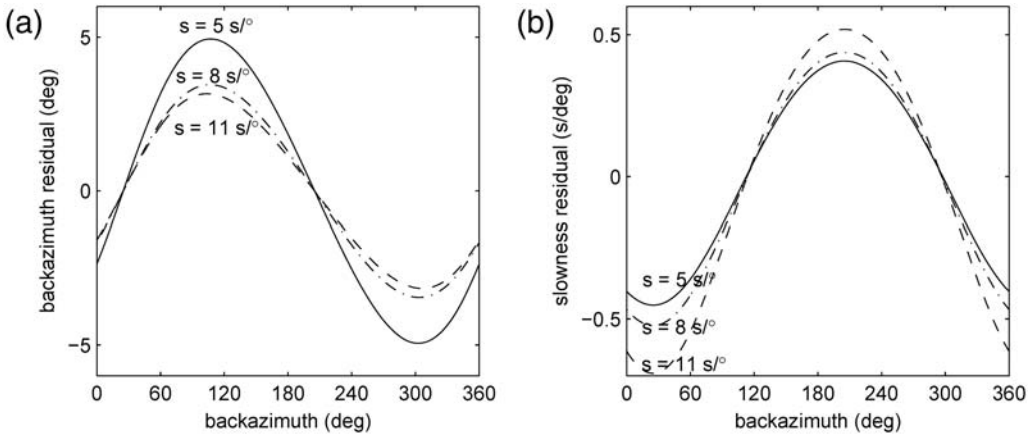

Figure 2. (a) Back-azimuth residuals and (b) slowness residuals for the model proposed by Hao and Zheng (2010)with a dip angle of 9°, a down-dip direction of N25°E, and a *P*-wave velocity of 6.8 km/s above the interface and 8.06 km/s below the interface. The incidence angles are taken to be 21°, 35°, and 53°, corresponding to the theoretical slowness values of 5, 8, and 11 s/°.

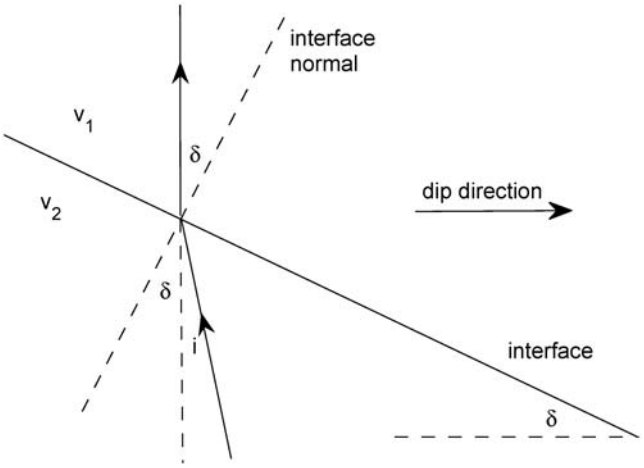

Figure 3. Drawing of vertically transmitted ray.

and slowness (numerical tests show that the bias can be up to 17°, 9°, and 5° in back azimuth and 1.4 s/°, 1.2 s/°, and 0.9 s/° in slowness for the theoretical slowness of 5 s/°, 8 s/°, and 11 s/°). The biased estimation may further lead to a biased dipping interface. To estimate the back-azimuth and slowness deviations accurately, it is suggested to take into account the vertical slowness during the slowness estimation as Bokelmann (1995) did for the GERESS array or make static corrections before the slowness estimation as Lindquist *et al.* (2007) and Tibuleac and Stroujkova (2009) did. Thirdly, one may notice that there are some discrepancies between the simulated results shown in our Figure 4 and the observed results shown in figure 4 of Hao and Zheng (2010), especially for the slowness deviations. The foregoing two points, as well as the point discussed in the next paragraph, may be responsible for these discrepancies. Another possible reason, as pointed out by Hao and Zheng (2010), is the limited resolution of the small-aperture LZDM array.

Regarding the reality of the large-dip Moho model, it is well known that the northeastern margin of the Tibetan plateau where lies the LZDM array is tectonically active and heavily deformed, and the possibility of a local northeast-dipping Moho beneath the LZDM array cannot be absolutely excluded. However, the presence of a northeast-dip Moho beneath the Lanzhou area is in contradiction to the studies of explosion seismology and receiver functions, which revealed a southwest-dipping Moho (e.g., Li *et al.*, 2002; Chen *et al.*, 2005; Zhao *et al.*, 2005; Liu *et al.*, 2006). The northeast-dip Moho model is more or less unconvincing if no other evidence is provided, especially when a 57° dip angle is concerned. It is easier to accept if we assume that the large-dip interface is located in the shallow crust because similar results have been reported previously. For instance, from the receiver function migration imaging of the eastern-most Qaidam–Kunlun boundary in the Northeast Tibetan plateau that is more than 600 km away from the LZDM array to the west, Shi *et al.* (2009) found a north-dip interface with a dip of 54° ± 9° in the upper crust. We find one possible solution for the identification of the depth location of the dipping interface through analysis of the back-azimuth and slowness deviations of seismic phases sampling different depth ranges. If the seismic phases that sample the shallow crust (e.g., *Pg*) show similar magnitudes of deviations in back azimuth and slowness to the seismic phases sampling deeper structure (e.g., *Pn* and teleseismic *P*), the dipping interface is preferably located in the shallow crust. Another candidate method is to estimate the back-azimuth and slowness deviations for seismic waves at lower frequencies, the wavelength of which is long enough to be insensitive to the shallow structures. If the deviations are still significant, the interface at deeper depth (e.g., the Moho) should be responsible.

Data and Resources

All data used in this article come from the published sources listed in the reference list.

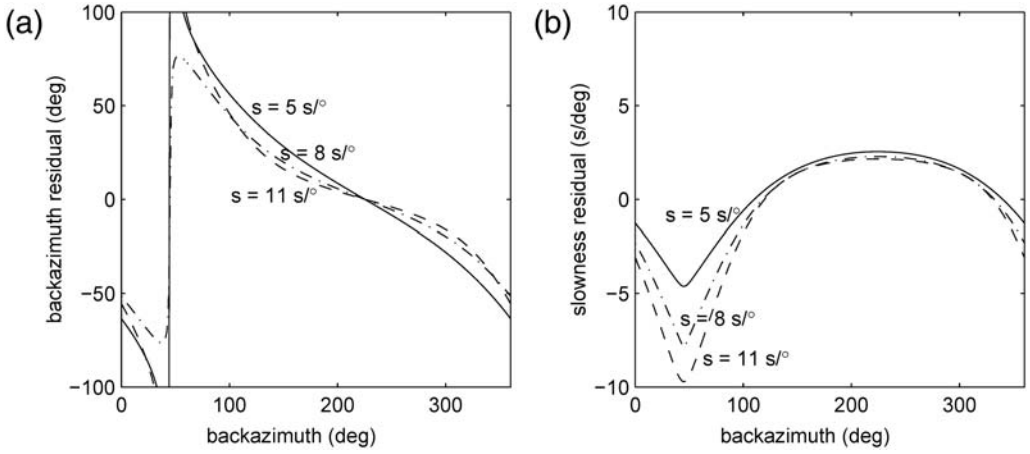

Figure 4. (a) Back-azimuth residuals and (b) slowness residuals for the large-dip model, with a dip angle of 57°, a down-dip direction of N45°E, and other parameters the same as those in Figure 2.

Acknowledgments

This study benefited from discussions with Jiuhui Chen. Special thanks to Diane Doser for her review and her suggestions that improved the manuscript. This study was supported by the Key Projects of Chinese National Programs for Fundamental Research and Development (Grant No. 2004CB418402).

References

Bokelmann, G. H. R. (1995). Azimuth and slowness deviations from the GERESS regional array, *Bull. Seismol. Soc. Am.* **85,** 1456–1463.

Chen, J. H., Q. Y. Liu, S. C. Li, B. Guo, and Y. G. Lai (2005). Crust and upper mantle *S*-wave velocity structure across Northeastern Tibetan Plateau and Ordos block, *Chinese J. Geophys.* **48,** 333–342 (in Chinese).

Hao, C., and Z. Zheng (2010). *P*-wave back-azimuth and slowness anomalies observed by an IMS seismic array LZDM, *Bull. Seismol. Soc. Am.* **100,** 657–669.

Koch, K., and U. Kradolfer (1997). Investigation of azimuth residuals observed at stations of the GSETT-3 Alpha network, *Bull. Seismol. Soc. Am.* **87,** 1576–1597.

Li, S. L., X. K. Zhang, C. K. Zhang, J. R. Zhao, and S. X. Cheng (2002). A preliminary study on the crustal velocity structure of Maqin-Lanzhou-Jingbian by means of deep seismic sounding profile, *Chinese J. Geophys.* **45,** 210–217 (in Chinese).

Lindquist, K. G., I. M. Tibuleac, and R. A. Hansen (2007). A Semiautomatic Calibration Method Applied to a Small-Aperture Alaskan Seismic Array, *Bull. Seismol. Soc. Am.* **97,** 100–113.

Liu, M., W. D. Mooney, S. Li, N. Okaya, and S. Detweiler (2006). Crustal structure of the northeastern margin of the Tibetan plateau from the Songpan-Ganzi terrane to the Ordos basin, *Tectonophysics* **420,** 253–266.

Niazi, M. (1966). Corrections to apparent azimuths and travel-time gradients for a dipping Mohorovicic discontinuity, *Bull. Seismol. Soc. Am.* **56,** 491–509.

Otsuka, M. (1966). Azimuth and slowness anomalies of seismic waves measured on the central California seismographic array. Part II: Interpretation, *Bull. Seismol. Soc. Am.* **56,** 655–675.

Shi, D., Y. Shen, W. Zhao, and A. Li (2009). Seismic evidence for a Moho offset and south-directed thrust at the easternmost Qaidam-Kunlun boundary in the Northeast Tibetan plateau, *Earth Planet. Sci. Lett.* **288,** 329–334.

Tibuleac, I. M., and A. Stroujkova (2009). Calibrating the Chiang Mai seismic array (CMAR) for improved event location, *Seism. Res. Lett.* **80,** 579–590.

Xu, J., Y. Zhao, X. Su, and T. Lv (2006). The site survey for Dajian Mountain seismic array in Lanzhou, *Seismol. Geomagn. Obs. Res.* **27,** (Suppl), 51–57 (in Chinese).

Zhao, J. R., S. L. Li, X. K. Zhang, Z. X. Yang, and C. K. Zhang (2005). Three dimensional Moho geometry beneath the northeast edge of the Qinghai-Tibet Plateau, *Chinese J. Geophys.* **48,** 78–85 (in Chinese).

State Key Laboratory of Earthquake Dynamics
Institute of Geology
China Earthquake Administration
Chaoyang District
Beijing 100029, China
lileipku00@gmail.com

Manuscript received 20 September 2010